Amyloid-like interactions within nucleoporin FG hydrogels

Christian Ader[a,1], Steffen Frey[b,1], Werner Maas[c], Hermann Broder Schmidt[b], Dirk Görlich[b,2], and Marc Baldus[a,2]

[a]Bijvoet Center for Biomolecular Research, Utrecht University, 3584 CH Utrecht, The Netherlands; [b]Department of Cellular Logistics, Max Planck Institute for Biophysical Chemistry, 37077 Göttingen, Germany; and [c]Bruker Biospin Corporation, 15 Fortune Drive, Billerica, MA 01821

Edited by Tom A. Rapoport, Harvard Medical School/HHMI, Boston, MA, and approved January 15, 2010 (received for review September 4, 2009)

The 62 kDa FG repeat domain of the nucleoporin Nsp1p forms a hydrogel-based, sieve-like permeability barrier that excludes inert macromolecules but allows rapid entry of nuclear transport receptors (NTRs). We found that the N-terminal part of this domain, which is characterized by Asn-rich inter-FG spacers, forms a tough hydrogel. The C-terminal part comprises charged inter-FG spacers, shows low gelation propensity on its own, but binds the N-terminal part and passivates the FG hydrogel against nonselective interactions. It was previously shown that a hydrophobic collapse involving Phe residues is required for FG hydrogel formation. Using solid-state NMR spectroscopy, we now identified two additional types of intragel interactions, namely, transient hydrophobic interactions between Phe and methyl side chains as well as intermolecular β-sheets between the Asn-rich spacer regions. The latter appear to be the kinetically most stable structures within the FG hydrogel. They are also a central feature of neuronal inclusions formed by Asn/Gln-rich amyloid and prion proteins. The cohesive properties of FG repeats and the Asn/Gln-rich domain from the yeast prion Sup35p appear indeed so similar to each other that these two modules interact *in trans*. Our data, therefore, suggest a fully unexpected cellular function of such interchain β-structures in maintaining the permeability barrier of nuclear pores. They provide an explanation for how contacts between FG repeats might gain the kinetic stability to suppress passive fluxes through nuclear pores and yet allow rapid NTR passage.

Beta-sheet | nuclear pore complex | Nup | Prion | solid-state NMR

Nuclear pore complexes (NPCs) control all nucleocytoplasmic exchange (1–4). Their permeability barrier allows free passage of small molecules but suppresses the flux of macromolecules larger than 30 kDa and thereby prevents an uncontrolled intermixing of nuclear and cytoplasmic contents. However, the permeability barrier also permits a rapid passage of even large cargoes, provided these are bound to appropriate nuclear transport receptors (NTRs) (2–5). NTRs thereby supply nuclei with proteins and the cytoplasm with ribosomes and other nuclear products.

FG repeat domains are essential building blocks of NPCs (6). They are considered to be natively unfolded and contain up to 50 repeat units, in which a characteristic hydrophobic patch, typically with the sequence FG, FxFG, or GLFG, is surrounded by more hydrophilic spacer sequences (7–9). These hydrophobic patches transiently bind NTRs during facilitated NPC passage (10–15).

Recent evidence suggests that the permeability barrier is a hydrogel derived from FG repeat domains (FG hydrogel) (13, 15–18). FG hydrogels have been predicted by the selective phase model (15, 16, 19) and indeed have been reconstituted from the FG/FxFG domain of the yeast nucleoporin Nsp1p (13, 16) or the GLFG domains from Nup49p and Nup57p (17). All these gels showed permeability properties very similar to those of NPCs themselves: they allowed an up to 20,000-fold faster entry of large NTR•cargo complexes than of the respective cargo alone. Within the ~600 residues FG/FxFG repeat domain of Nsp1p ($FG/FxFG^{Nsp1p}_{2-601}$), phenylalanines are critical not only for NTR binding, but also for gel formation (13), suggesting that interrepeat contacts involve some form of hydrophobic interaction.

According to the selective phase model, FG hydrogels are reversibly cross-linked three-dimensional protein meshworks, whose mesh size determines their size-exclusion limit for inert objects. NPCs already significantly restrict the flux of GFP-sized objects (diameter ≈ 5 nm) (19, 20). NTR•cargo complexes, however, are typically much larger than GFP and thus exceed the expected mesh size. Yet they cross NPCs in a facilitated manner. This implies that interrepeat contacts dissociate rapidly in the vicinity of an NTR but are kinetically stable elsewhere in the gel (16). To understand this phenomenon, we foremost need structural information on FG repeat interactions. As gels are intrinsically disordered and not soluble, such information is difficult to obtain by X-ray crystallography or solution NMR. Solid-state NMR (ssNMR), however, proves to be the ideal technique to study both formation and structural organization of an FG hydrogel.

Results

The Nsp1 FG/FxFG Hydrogel Contains Rigid and Dynamic Segments. To probe mobile as well as rigid segments of a fully carbon (^{13}C), nitrogen (^{15}N) isotope-labeled FG hydrogel derived from the complete Nsp1 FG/FxFG repeat domain ($FG/FxFG^{Nsp1p}_{2-601}$) in a complementary manner, we acquired two-dimensional (^{13}C-^{13}C) correlation spectra employing through-space and through-bond mixing units (21, 22) (Fig. 1*A*, *B*). Even without sequential resonance assignments for this 62 kDa protein domain, NMR line widths, peak positions, and the overall correlation patterns clearly distinguish dynamically different protein segments (Fig. S1). The established standard amino acid-specific peak positions (23) were used to approximate the relative distribution of amino acids within the rigid and the mobile segments (Fig. 1*C*). The mobile, unstructured segments contain large fractions of the charged amino acids Asp, Glu, and Lys. They occur foremost in the highly regular and charged inter-FG spacers of the C-terminal part of the FG/FxFG repeat domain ($FSFG^{Nsp1p}_{274-601}$; Fig. 1*D* and Fig. S2). In contrast, Thr, Asn, and Gln are typical of the NQTS-rich inter-FG spacers most prominently found within the N-terminal part of the FG/FxFG domain (FG^{Nsp1p}_{2-175}; Fig. 1*D* and Fig. S2). They characterize the rigid segments and might thus act as anchoring points of the gel network. This is striking because so far only hydrophobic interactions, especially those involving Phe, have been considered to stabilize an FG hydrogel (13, 15, 19). Phe residues, however, appear to reside balanced between both motional regimes. This

Author contributions: C.A., S.F., D.G., and M.B. designed research; C.A., S.F., and H.B.S. performed research; W.M. contributed new reagents/analytic tools; C.A., S.F., D.G., and M.B. analyzed data; and C.A., S.F., D.G., and M.B. wrote the paper.

The authors declare no conflict of interest.

This article is a PNAS Direct Submission.

Freely available online through the PNAS open access option.

[1]C.A. and S.F. contributed equally to this work.

[2]To whom correspondence may be addressed. E-mail: goerlich@mpibpc.mpg.de or m.baldus@uu.nl.

This article contains supporting information online at www.pnas.org/cgi/content/full/0910163107/DCSupplemental.

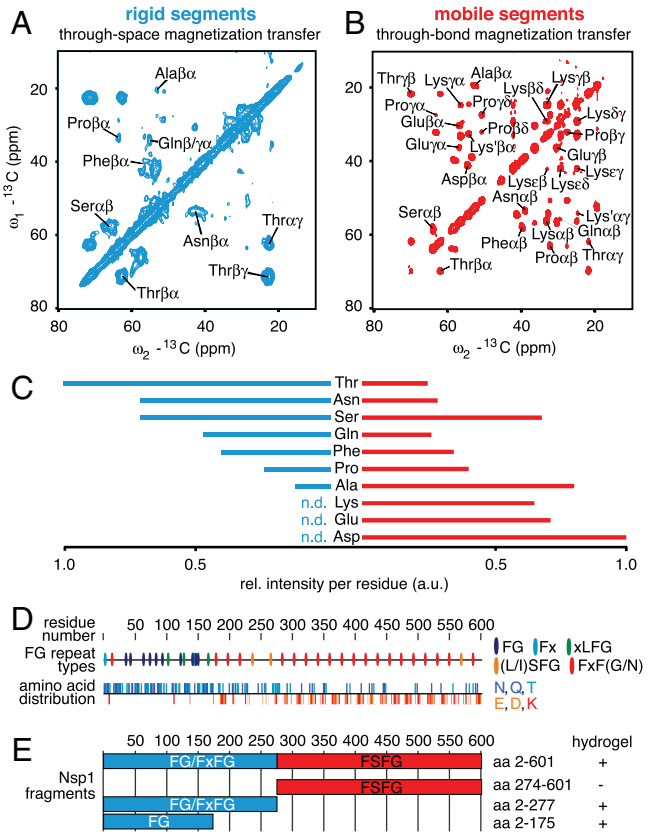

Fig. 1. The Nsp1 FG/FxFG domain contains rigid and mobile segments. (*A*), (*B*) Investigation of rigid and mobile segments of the Nsp1 hydrogel using 2D (^{13}C-^{13}C) ssNMR employing through-space (*A*) and through-bond (*B*) mixing. Amino acid-specific assignments are indicated. (*C*) Relative (rel.) Cα-Cβ peak intensities per residue obtained from both spectra allow one to estimate the amino acid distribution within the rigid (left, blue) and mobile (right, red) segments of the hydrogel (n.d.: no Cα-Cβ peak detected). (*D*) Linear representations illustrating the nonuniform distribution of the various FG repeat types (*Top*) and relevant amino acids (*Bottom*) within the FG/FxFG$^{Nsp1p}_{2–601}$ domain. (*E*) Bar models of Nsp1p fragments with high and low gel-forming propensity as determined by qualitative gelation assays (Table S1).

might reflect the paradox that interrepeat contacts must be kinetically stable enough to pose a firm barrier while, at the same time, phenylalanines must rapidly bind approaching NTRs and transmit the signal for opening a mesh.

The Nsp1 FG/FxFG Repeat Hydrogel Is Stabilized by Hydrophobic Interactions and by Amyloid-Like Interchain β-Sheets. Line widths and peak positions (23) in the NMR spectrum employing scalar-based polarization transfer indicate that mobile segments are largely unstructured (Fig. 1*B*). This is supported by the occurrence of only very few interresidue cross-peaks in proton-proton (^{1}H-^{1}H) NOESY (24) spectra obtained under magic angle spinning (Fig. S3), even at long contact times. Because of limited spectral dispersion and the large size of the repeat domain, Phe-Phe interactions proposed previously to stabilize the hydrogel as well as other interactions between identical side chains could not be resolved by two-dimensional NMR. Strikingly, however, the NOESY spectra of both full length and N-terminal Nsp1 hydrogels revealed spatial vicinity between aliphatic side chain protons and the aromatic ring protons of Phe (Fig. 2*A*). These hydrophobic interactions of Phe and aliphatic side chains most likely occur on a dynamic and transient level (Fig. 2*A*). Nevertheless, they appear essential for gelation, because mutant FG repeat domains lacking hydrophobic residues also fail to form hydrogels (Table S1) (see also ref. 13).

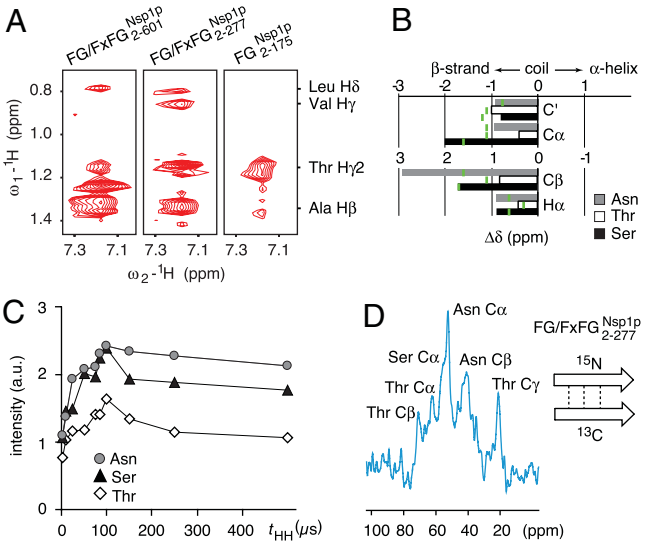

Fig. 2. NMR characterization of Nsp1 hydrogel structure and gelation. (*A*) Details of NOESY spectra obtained for indicated Nsp1p fragments (250 ms mixing time) showing interresidue cross-peaks between indicated side chain methyls and Phe side chains. (*B*) Bar graph of C′, Cα, Cβ, and Hα chemical-shift differences for resonances of rigid Asn, Thr, and Ser of FG/FxFG$^{Nsp1p}_{2–601}$ as compared to statistical average values for β-strands (green lines). (*C*) Dependence of Cα peak intensities for Asn, Thr, and Ser on the ^{1}H-^{1}H mixing time (t_{HH}) in NHHC (25) experiments suggests NH-HCα proton-proton distances compatible with β-strands. (*D*) NHHC spectrum obtained for a hydrogel containing ^{13}C-labeled FG/FxFG$^{Nsp1p}_{2–277}$ and ^{15}N-labeled FG/FxFG$^{Nsp1p}_{2–277}$ at a 1:1 ratio. The signal arises due to short ^{1}H-^{1}H distances between complementary labeled β-strands forming an intermolecular sheet (see sketch and *Materials and Methods* for details).

C′, Cα, Cβ, and Hα chemical shifts are very sensitive to secondary structure elements (23). They concordantly point towards a β-strand backbone conformation within rigid NQTS-rich spacers (Fig. 2*B* and Fig. S4). In such conformations, sequential NH-Hα proton-proton distances should be short (2–3 Å), which is in line with the observed rapid magnetization transfer (maximum intensities at 100 μs ^{1}H-^{1}H mixing) from amide nitrogen atoms to the alpha carbons via directly bonded ^{1}H spins (25) (Fig. 2*C*). Similar nitrogen-carbon correlation experiments (26) performed on a 1:1 mixture of ^{15}N- and ^{13}C-labeled probes further revealed that individual FG/FxFG$^{Nsp1p}_{2–277}$ chains interact *in trans*, with proton-proton distances of less than 5 Å (Fig. 2*D*). This demonstrates that the detected β-strands (Fig. 2*B*, *C*) form interchain β-sheets and further suggests that these sheets constitute a major structural element of the FG hydrogel. Fig. S5 shows structural models for the interaction between NQTS-rich motifs of the FG hydrogel that are compatible with our ssNMR data.

The FG/FxFG repeat domain from Nsp1p forms an FG hydrogel with permeability properties that resemble closely those of intact NPCs (16). Our finding that intermolecular β-sheets between NQTS-rich sequences are the most stable intragel structures is so striking because similar interchain β-sheets are also the structural hallmark of amyloid fibrils (27, 28). Already in the year 2000, certain Nups had been recognized as NQ-rich (29) and thereby as related to NQ-rich amyloid-forming proteins like glutamine-extended variants of huntingtin (30) or the yeast prion Sup35p (31). More recently, cellular assays revealed that several nucleoporins containing NQ-rich domains exhibit amyloid-like characteristics in vivo (32). However, this has so far not been linked to a cellular function.

The Gelation Propensity of Nsp1 FG Repeats Correlates with the Occurrence of NQTS-Rich Spacers. The NQTS-rich inter-FG spacers of the Nsp1 FG/FxFG repeat domain are concentrated within the

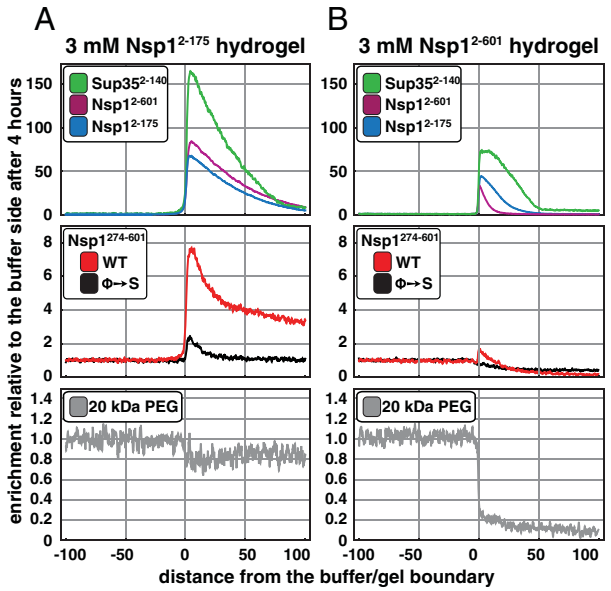

Fig. 3. FG^{Nsp1p}_{2-175}, $FxFG^{Nsp1p}_{274-601}$, and the N/Q-rich Sup35 prion domain specifically interact with Nsp1-derived hydrogels. (*A*) Hydrogel droplets containing 3 mM of the FG^{Nsp1p}_{2-175} repeat domain were incubated with 2 μM of the indicated Atto488-labeled species (0.5 μM for $Sup35^{2-140}$). After 4 h, partitioning of the fluorescent species between buffer and gel phases was analyzed. Note that the full-length repeat domain ($Nsp1^{2-601}$) and the N-terminal portion with the highest gel-forming propensity ($Nsp1^{2-175}$) interacted strongly with the hydrogel. The prion domain of Sup35p ($Sup35^{2-140}$) showed an even higher partitioning into the gel phase. In comparison to a corresponding mutant repeat domain lacking all hydrophobic residues ($Nsp1^{274-601}$ Φ→S) or a 20 kDa PEG polymer, also $FxFG^{Nsp1p}_{274-601}$ was considerably enriched within the FG^{Nsp1p}_{2-175} hydrogel. (*B*) Hydrogels with 3 mM $FG/FxFG^{Nsp1p}_{2-601}$ were analyzed exactly as in (*A*). In comparison to the FG^{Nsp1p}_{2-175} hydrogel, the inclusion of the $FSFG^{Nsp1p}_{176-601}$ module into the gel not only blocked binding sites for fluorescent $FSFG^{Nsp1p}_{274-601}$ molecules (*Middle*), but also efficiently suppressed influx and partitioning of the inert PEG control polymer into the gel (*Lower*).

N-terminal 175 residues (Fig. 1*D* and Fig. S2). If the rigid, amyloid-like segments seen by ssNMR spectroscopy were crucial for hydrogel stability, then the isolated N-terminal part (FG^{Nsp1p}_{2-175}) should show a greater gelation propensity than the C-terminal part ($FSFG^{Nsp1p}_{274-601}$), whose spacers are charged and not NQTS-rich. Indeed, FG^{Nsp1p}_{2-175} and $FG/FxFG^{Nsp1p}_{2-277}$ formed strong hydrogels (Table S1 and Fig. 1*E* and see below Figs. 3*A* and 4*A*), while the isolated C-terminal repeats remained liquid under identical conditions. The fact that NQTS-rich spacers are also typical of the FG repeats from Nup100p, Nup116p, Nup49p, and Nup57p (Tables S2, S3) provides a plausible explanation as to why these repeats appear particularly cohesive (17, 18).

NQTS-Rich FG Repeats Interact with the Canonical NQ-Rich Amyloid Domain from the Yeast Prion Sup35p. Residues 2-140 from the yeast prion Sup35p represent the prototypical example of an amyloid-forming NQ-rich domain (31). Our ssNMR data suggest that NQTS-rich FG repeats contact each other through intermolecular β-sheets similar to those observed between individual Sup35p molecules. We therefore wondered if this intriguing similarity reaches so far as to allow heterotypic interactions between FG repeats and the NQ-rich Sup35 prion domain. To test this, we prepared hydrogels from the N-terminal (FG^{Nsp1p}_{2-175}) or the complete Nsp1 FG/FxFG domain ($FG/FxFG^{Nsp1p}_{2-601}$) and added fluorescently labeled $Sup35^{2-140}$ to the buffer sides (Fig. 3*A* and *B*, *Upper*). Indeed, 4 h later, we found the prion domain ≈ 100-fold enriched within the FG hydrogels. In fact, $Sup35^{2-140}$ partitioned

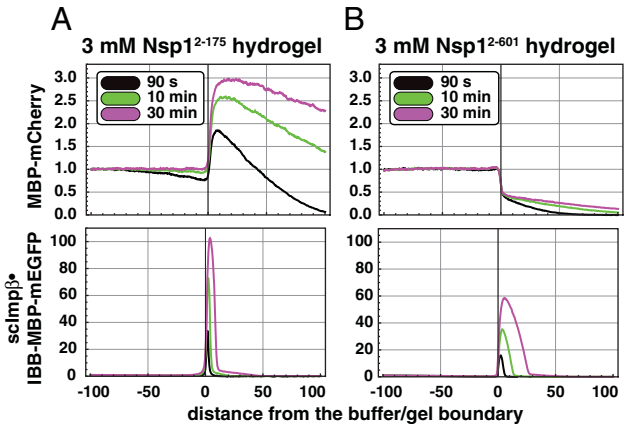

Fig. 4. The charged FSFG repeat domain facilitates entry of NTR • cargo complexes and passivates the hydrogel against nonspecific binding of inert proteins. Hydrogels consisting of 3 mM of the indicated repeat domains were formed as in Fig. 3. Influx of MBP-mCherry or an IBB-MBP-mEGFP•scImpβ complex into these hydrogels was analyzed after 90 sec, 10 min, and 30 min. Note that the intragel movement of IBB-MBP-mEGFP•scImpβ within the FG^{Nsp1p}_{2-175} hydrogel was about 3-fold slower than in the $FG/FxFG^{Nsp1p}_{2-601}$ hydrogel, while the enrichment of the NTR•cargo complexes at the buffer/gel boundary was increased by a factor of 2. The presence of the more C-terminal FxFG repeats harboring charged spacers also significantly reduced nonspecific binding of inert proteins to the hydrogels.

from the buffer even more efficiently into the FG hydrogels than the Nsp1-derived FG repeats we used as positive controls (Fig. 3*A* and *B*, *Upper*). Thus, NQTS-rich FG repeats and $Sup35^{2-140}$ can act as complementary binding partners, which in turn suggests that the interaction between NQTS-rich FG repeats must indeed be very similar to interactions between such canonical NQ-rich amyloid domains.

The N-Terminal Amyloid-Like FG Repeats of Nsp1p Interact with the Charged C-Terminal Part to Form a Highly Selective Barrier. The charged $FSFG^{Nsp1p}_{274-601}$ fragment alone is unable to form a hydrogel (Fig. 1*E* and Table S1) and lacks an amyloid-type sequence feature (Fig. S2). This poses the question of how far it interacts with other FG repeats and contributes to the hydrogel-based permeability barrier. Fig. 3*A*, *Middle*, shows that fluorescently labeled $FSFG^{Nsp1p}_{274-601}$ interacts with the N-terminal repeats and enriches 8-fold within the $FSFG^{Nsp1p}_{2-175}$ hydrogel. Several controls verified the specificity of this effect. First, a 20 kDa PEG labeled with the same fluorescent dye was not enriched (Fig. 3*A*, *Lower*). Second, mutating the hydrophobic residues (Phe, Leu, Val, Ile) of $FSFG^{Nsp1p}_{274-601}$ to serines (Φ→S mutant) greatly weakened the interaction (Fig. 3*A*, *Middle*), which is consistent with the notion of hydrophobic interactions driving interrepeat contacts. Third, the binding was saturable: $FSFG^{Nsp1p}_{274-601}$ partitioned only weakly into a gel that comprised the complete FG/FxFG repeat domain and thus already contained $FSFG^{Nsp1p}_{274-601}$ as an internal, covalently linked competitor (compare Fig. 3*A* and *B*, *Middle panels*).

Including the charged $FSFG^{Nsp1p}_{274-601}$ repeats as part of the full-length FG/FxFG domain improved the selectivity of the hydrogel. First, it lowered the gel/buffer partition coefficient of the PEG marker from ≈0.8 to ≈0.2 (compare *Lower panels* Fig. 3*A* and *B*). Since the number of 0.2 is far below the expected volume fraction for the bulk solvent, this suggests a greatly improved sieving effect. Second, the $FSFG^{Nsp1p}_{2-175}$ hydrogel showed an unexpected affinity for certain inert cargoes and enriched e.g. an MBP-mCherry fusion ≈3-fold (Fig. 4*A*, *Upper*). This "incorrect" selectivity was fully suppressed in the full-length gel, i.e. when the charged

$FSFG^{Nsp1p}_{274-601}$ repeats were part of the gel (Fig. 4*B*, *Upper*). Third, the presence of the C-terminal repeats also allowed an importin β●cargo complex to diffuse considerably faster from the buffer/gel boundary into the gel (compare *Lower panels* of Fig. 4*A* and *B*).

So far, we only implied two requirements for an FG repeat-based permeability barrier: a sieve-like structure with meshes small enough to exclude inert objects larger than ≈5 nm in diameter as well as facilitated entry of NTRs. We now observed a third requirement, namely, "passivation" of FG repeats against binding of macromolecules other than NTRs. Nsp1p acts in that like a two-component system: the N-terminal repeats show a very high gelation propensity but need to be "passivated" by the highly charged FSFG repeats found in the C-terminal part of the repeat domain. This supports the notion that heterogeneity in FG repeat sequences is advantageous for the performance of the NPC permeability barrier. Interestingly, FG hydrogels comprising only GLFG repeats from Nup49p and Nup57p exclude inert proteins already well without the need of charged spacers (17), suggesting that several optimal solutions for the just discussed passivation problem exist.

FG Hydrogel Formation Proceeds Through Two Successive Steps. Using ssNMR, we have detected rigid β-structures within the Nsp1 FG hydrogel. If these structures were crucial for stabilizing the hydrogel, then they should appear during gelation. Using a custom-designed ssNMR probehead, we were able to simultaneously track changes in translational diffusibility of the full length Nsp1 FG/FxFG repeat domain using pulsed-field gradients (PFG) and monitor the occurrence of immobilized protein species using cross-polarization (CP) experiments (Fig. 5). The effective diffusion coefficient was derived from the PFG experiments (Fig. S6) and decreased steeply during the first 30 min of gelation from a starting value of 1.7×10^{-10} m^2/s (as expected for monomeric $FG/FxFG^{Nsp1p}_{2-601}$), over almost 3 orders of magnitude (Fig. 5), indicating formation of assemblies of increasing size. Interestingly, this process largely preceded the emergence of rigid β-sheet structures detected by the CP signal (Fig. 5). Rigid structures became apparent only after 30 min, suggesting that decrease in diffusibility and formation of β-sheet segments are two consecutive steps during gelation. This behavior is reminiscent of the kinetic lag phase observed during amyloid formation (33). In vivo, however, gelation is expected to occur more rapidly, possibly through the catalytic action of NTRs.

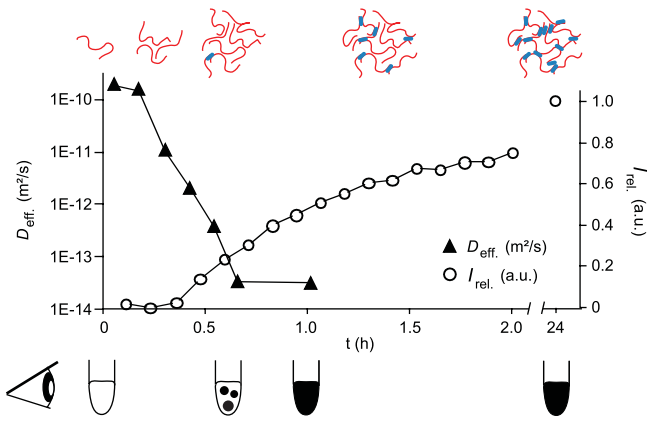

Fig. 5. Comparison of the time-dependent decrease of the effective diffusion coefficient D_{eff} extracted from the PFG experiments (▲, logarithmic scale) and of the buildup of cross-polarization signals reflecting β-strands (○). Lines are drawn to guide the eye. The cartoon at the top illustrates the initial formation of protein clusters and the appearance of rigid β-strands. The bottom cartoon depicts formation of the gel (black) as followed by visual inspection of $FG/FxFG^{Nsp1p}_{2-601}$ (as used for NMR).

In conclusion, the failure of the Φ→S mutants to form a hydrogel (Table S1) (see also ref. 13) and the data obtained by structural and kinetic ssNMR suggest that both, rather dynamic hydrophobic as well as rigid hydrophilic, amyloid-type interactions stabilize the investigated FG hydrogel. Based on these findings, it is tempting to interpret the two observed stages of gelation as an initial hydrophobic collapse leading to high molecular weight clusters, which are subsequently stabilized by intermolecular hydrogen-bond interactions within β-sheets.

Discussion

Comparison of the Nsp1 Hydrogel with NQ-Rich Amyloids. The NQTS-rich sequences of nucleoporins connect FG motifs in a repeat domain. In contrast to previous belief, they are, however, not just functionless spacers. Instead, they engage in amyloid-like protein-protein contacts that presumably tighten the FG hydrogel-based permeability barrier of NPCs. Such a fundamental cellular function for amyloid-type interactions would indeed be remarkable, because amyloids are commonly linked to pathological conditions, such as Huntington's, Alzheimer's, or Parkinson's disease (27). It is only beginning to emerge that amyloids also have a functional relevance (27, 34). NPCs might be another striking example of that.

NQ-rich amyloids and the FG hydrogel analyzed here are both stabilized by a characteristic type of β-structures. These structures are not part of a globular fold and connect distinct polypeptide chains to large macromolecular assemblies. In both cases, NQ-rich sequences contribute to the interaction. The cohesiveness of the NQTS-rich FG repeats appears to be so akin to that of the NQ-rich prion domain of Sup35p that the two modules interact with each other. Apart from these striking similarities, there are also crucial differences. First, FG repeats bind NTRs, while e.g. the prion domain of Sup35p does not, obviously because the hydrophobic residues in the prion domain are tyrosines that cannot be accommodated into the FG binding sites of NTRs (10, 13). Second, NQ-rich amyloids are very dense, tightly packed structures, where side chain stacking generates an additional anhydrous peptide interface between the β-sheets (35). How far side chain stacking contributes also to inter-FG repeat contacts is as yet unclear. However, FG hydrogel formation apparently stops before a complete collapse of the structure. Consequently, FG hydrogels include water and allow passive entry of small molecules and facilitated entry of NTRs.

Too strong inter-FG repeat interactions might be counteracted by the presence of residues that form weaker β-sheets than Gln, such as Ser or Gly. Likewise, the charged C-terminal FxFG repeats of Nsp1p apparently modulate the gel strength such that NTRs can move ≈3-fold faster through the gel (see Fig. 4).

A Model That Incorporates Amyloid-Like Interactions into NPC Function. In contrast to pathological amyloids, inter-FG repeat contacts do not result in irreversible aggregates. Instead, FG hydrogels are easily traversed by NTRs and their cargo complexes (16, 17). How might this work? The key to the solution might be that interrepeat contacts comprise two elements, namely, hydrophobic interactions between FG clusters as well as β-sheets between the NQTS-rich spacers. Such composite contacts appear sufficiently stable to suppress fluxes of large inert material. Thermal breathing should transiently expose mobile FG motifs and allow an approaching NTR to bind (Fig. 6). Although the hydrophobic intragel interactions may be transient, they apparently control the association state of the β-strand segments and render them kinetically stable. This is nicely illustrated by mutant FG repeat domains that lacks hydrophobic residues and consequently fail to form a gel (Table S1) (see also ref. 13). Sequestering a hydrophobic FG cluster by an NTR might therefore also open

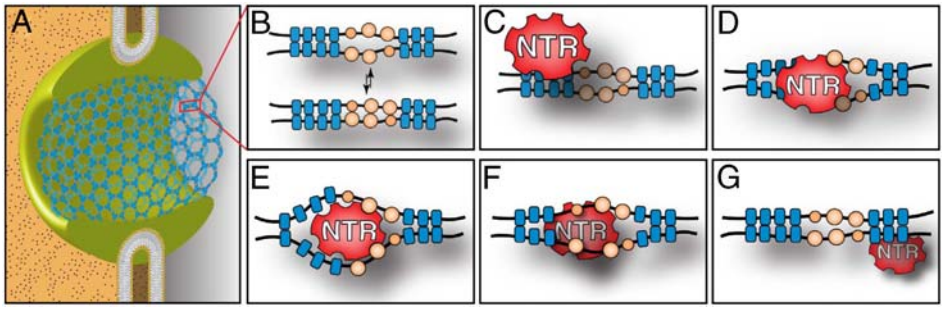

Fig. 6. Illustration of how an NTR might catalyze its own passage through an NQ-rich inter-FG repeat contact. (*A*) Drawing of an NPC filled with a schematized FG hydrogel. (*B*) Interrepeat contacts comprise rigid intermolecular β-sheets between NQTS-rich spacers (blue) and essential hydrophobic interactions between FG motifs (orange). The sum of interactions confers kinetic stability to these contacts, despite rapid fluctuations within the hydrophobic interactions. The energy barrier for dissociating such interrepeat contact should be lower when elementary interactions are broken not all at once but successively and if intermediates are stabilized by NTR-binding. (*C*–*G*) Binding of an NTR to FG motifs destabilizes and eventually dissociates the adjacent β-sheets, allowing the NTR to pass. The mesh contact is closed by the reverse reaction. Drawing is not to scale.

adjacent β-sheets and allow the NTR•cargo complex to pass (Fig. 6). Energetically, this can be seen as if the energy released by the FG•NTR interaction is spent on opening the β-sheet component of the interrepeat contact.

Materials and Methods

A detailed summary of our experimental procedures, including protein expression, hydrogel preparation, influx assays, and NMR experiments is given in the supplemental information, which also includes Figs. S1–S6, Tables S1–S4 and relevant references.

ACKNOWLEDGMENTS. We thank H. Behr and J. Schünemann for excellent technical help. C.A. received a fellowship of the Stiftung Stipendien-Fonds des Verbands der Chemischen Industrie. This work was funded in part by the Max-Planck-Gesellschaft and the Netherlands Organization for Scientific Research (Grant 700.26.121).

1. D'Angelo MA, Hetzer MW (2008) Structure, dynamics and function of nuclear pore complexes. *Trends Cell Biol* 18:456–466.
2. Fried H, Kutay U (2003) Nucleocytoplasmic transport: Taking an inventory. *Cell Mol Life Sci* 60:1659–1688.
3. Görlich D, Kutay U (1999) Transport between the cell nucleus and the cytoplasm. *Annu Rev Cell Dev Biol* 15:607–660.
4. Macara IG (2001) Transport into and out of the nucleus. *Microbiol Mol Biol Rev* 65:570–596.
5. Cook A, Bono F, Jinek M, Conti E (2007) Structural biology of nucleocytoplasmic transport. *Annu Rev Biochem* 76:647–671.
6. Strawn LA, Shen T, Shulga N, Goldfarb DS, Wente SR (2004) Minimal nuclear pore complexes define FG repeat domains essential for transport. *Nat Cell Biol* 6:197–206.
7. Denning DP, Patel SS, Uversky V, Fink AL, Rexach M (2003) Disorder in the nuclear pore complex: The FG repeat regions of nucleoporins are natively unfolded. *Proc Natl Acad Sci USA* 100:2450–2455.
8. Denning DP, Rexach MF (2007) Rapid evolution exposes the boundaries of domain structure and function in natively unfolded FG nucleoporins. *Mol Cell Proteomics* 6:272–282.
9. Rout MP, Wente SR (1994) Pores for thought: Nuclear pore complex proteins. *Trends Cell Biol* 4:357–365.
10. Bayliss R, Littlewood T, Stewart M (2000) Structural basis for the interaction between FxFG nucleoporin repeats and importin-beta in nuclear trafficking. *Cell* 102:99–108.
11. Bayliss R, et al. (1999) Interaction between NTF2 and xFxFG-containing nucleoporins is required to mediate nuclear import of RanGDP. *J Mol Biol* 293:579–593.
12. Bednenko J, Cingolani G, Gerace L (2003) Importin beta contains a COOH-terminal nucleoporin binding region important for nuclear transport. *J Cell Biol* 162:391–401.
13. Frey S, Richter RP, Görlich D (2006) FG-rich repeats of nuclear pore proteins form a three-dimensional meshwork with hydrogel-like properties. *Science* 314:815–817.
14. Iovine MK, Watkins JL, Wente SR (1995) The GLFG repetitive region of the nucleoporin Nup116p interacts with Kap95p, an essential yeast nuclear import factor. *J Cell Biol* 131:1699–1713.
15. Ribbeck K, Görlich D (2002) The permeability barrier of nuclear pore complexes appears to operate via hydrophobic exclusion. *EMBO J* 21:2664–2671.
16. Frey S, Görlich D (2007) A saturated FG-repeat hydrogel can reproduce the permeability properties of nuclear pore complexes. *Cell* 130:512–523.
17. Frey S, Görlich D (2009) FG/FxFG as well as GLFG repeats form a selective permeability barrier with self-healing properties. *EMBO J* 28:2554–2567.
18. Patel SS, Belmont BJ, Sante JM, Rexach MF (2007) Natively unfolded nucleoporins gate protein diffusion across the nuclear pore complex. *Cell* 129:83–96.
19. Ribbeck K, Görlich D (2001) Kinetic analysis of translocation through nuclear pore complexes. *EMBO J* 20:1320–1330.
20. Mohr D, Frey S, Fischer T, Güttler T, Görlich D (2009) Characterisation of the passive permeability barrier of nuclear pore complexes. *EMBO J* 28:2541–2553.
21. Andronesi OC, et al. (2005) Determination of membrane protein structure and dynamics by magic-angle-spinning solid-state NMR spectroscopy. *J Am Chem Soc* 127:12965–12974.
22. Siemer AB, et al. (2006) Observation of highly flexible residues in amyloid fibrils of the HET-s prion. *J Am Chem Soc* 128:13224–13228.
23. Wang Y, Jardetzky O (2002) Probability-based protein secondary structure identification using combined NMR chemical-shift data. *Protein Sci* 11:852–861.
24. Jeener J, Meier BH, Bachmann P, Ernst RR (1979) Investigation of exchange processes by two-dimensional NMR spectroscopy. *J Chem Phys* 71:4546–4553.
25. Lange A, Seidel K, Verdier L, Luca S, Baldus M (2003) Analysis of proton-proton transfer dynamics in rotating solids and their use for 3D structure determination. *J Am Chem Soc* 125:12640–12648.
26. Etzkorn M, Bockmann A, Lange A, Baldus M (2004) Probing molecular interfaces using 2D magic-angle-spinning NMR on protein mixtures with different uniform labeling. *J Am Chem Soc* 126:14746–14751.
27. Chiti F, Dobson CM (2006) Protein misfolding, functional amyloid, and human disease. *Annu Rev Biochem* 75:333–366.
28. Sunde M, Blake CCF (1998) From the globular to the fibrous state: Protein structure and structural conversion in amyloid formation. *Q Rev Biophys* 31:1–39.
29. Michelitsch MD, Weissman JS (2000) A census of glutamine/asparagine-rich regions: Implications for their conserved function and the prediction of novel prions. *Proc Natl Acad Sci USA* 97:11910–11915.
30. Bates G (2003) Huntingtin aggregation and toxicity in Huntington's disease. *The Lancet* 361:1642–1644.
31. DePace AH, Santoso A, Hillner P, Weissman JS (1998) A critical role for amino-terminal glutamine/asparagine repeats in the formation and propagation of a yeast prion. *Cell* 93:1241–1252.
32. Alberti S, Halfmann R, King O, Kapila A, Lindquist S (2009) A systematic survey identifies prions and illuminates sequence features of prionogenic proteins. *Cell* 137:146–158.
33. Harper JD, Lansbury PT (1997) Models of amyloid seeding in Alzheimer's disease and scrapie: Mechanistic truths and physiological consequences of the time-dependent solubility of amyloid proteins. *Annu Rev Biochem* 66:385–407.
34. Fowler DM, Koulov AV, Balch WE, Kelly JW (2007) Functional amyloid—from bacteria to humans. *Trends Biochem Sci* 32:217–224.
35. Nelson R, et al. (2005) Structure of the cross-beta spine of amyloid-like fibrils. *Nature* 435:773–778.